

B. E. Paton, L. M. Lobanov, V. V. Łysak, V. V. Knysz, V. I. Pavlovskij, V. P. Priluckij, A. N. Timoszenko, P. V. Gonczarov, Guan Cyao

## Strain-free Welding of VT-20 (BT-20) Stringer Panels

**Abstract:** The paper presents results of a complex of investigations on the development of technology of welding of stringer panels of titanium alloy using a slot weld, providing minimum residual stresses and strains and high values of their service life at cyclic loads. Welding of T-joints was performed by slot welds on full-scale specimens using three method of welding: electron beam, automatic non-consumable electrode argon arc welding along the layer of activating flux and automatic non-consumable electrode argon arc welding with immersed arc. To eliminate the residual welding stresses and strains the preliminary elastic deforming of elements being welded was applied. Testing of all the types of specimens for their fatigue at longitudinal cyclic tension was carried out. The effect of heat-treatment, peening mechanical treatment and repair-welding technologies on their fatigue life was also determined. On the basis of results of investigations of full-scale specimens the batches of stringer panels of 1200 mm length were manufactured and tested. It was found that making of slot welds by argon arc non-consumable electrode welding along the activating flux using preliminary elastic deforming and high-frequency mechanical peening provides the higher characteristics of fatigue life of welded stringer panels of high-strength titanium alloy VT-20 as compared with electron beam welding and argon arc non-consumable electrode welding with immersed arc. The developed technology can serve the basis for industrial manufacture of welded stringer panels of high-strength titanium alloys.

**Keywords:** stringer panels, titanium alloys, welding of T-joints

Light alloy stringer panels are becoming increasingly popular in aviation and space, shipbuilding and other industrial sectors. The leading aviation companies pay particular attention to creating new technologies and improving already existing ones for making supporting, thin-walled panels of high-strength titanium alloys. A characteristic example is the application of TIG-welded 2.5 mm thick and up to 2000 mm long stringer panels reinforced with up to 25 mm reinforcing ribs, made of VT-20 titanium alloy in multi-role aircraft manufactured by the Russian Sukhoi company. After welding panels placed in a fixing device made of stainless steel are subjected to annealing in an electric vacuum furnace in order to reduce internal stresses and plastic strains [1].

B. E. Paton, Academician; L.M. Lobanov, Academician at the National Academy of Sciences of Ukraine, V. V. Łysak, Eng.; V. V. Knysz, PhD (DSc) hab. Eng.; V. I. Pavlovskij PhD (DSc) Eng.; V. P. Priluckij, PhD (DSc) Eng.; A.N. Timoszenko, PhD (DSc) Eng.; P. V. Gonczarov MSc Eng. - E. O. Paton Electric Welding Institute, the National Academy of Sciences of Ukraine, Kiev; Guan Cyao Academician at Beijing Institute of Aircraft Technologies

At the NASA research centre in Langley, a weldbrazing method for making similar structures has been developed. By means of this method Z-like reinforcing ribs of titanium alloy are spot welded to a titanium sheet via aluminium brazing metal interpass. Next, such a structure of panels is placed in a vacuum chamber where the brazing process is conducted [1].

The structural elements of an F-14 military jet are made of electron beam welded titanium alloy. This material and technological (EBW) combination ensures both high joint quality and high efficiency [2].

Irrespective of whether the issue is related to structures made of titanium alloys or of other materials, the aviation industry technologists, while endeavouring to ditch thin-walled ribbed riveted or milled structures for structures with welded reinforcing ribs, encounter the problem of reducing the effect of such inconvenient factors as internal stresses and plastic strains. These factors, characteristic of welding processes, significantly deteriorate the functional properties of products, and particularly their precision and service life [3].

In order to improve the precision and fatigue properties of thin-walled welded structures, the E. O. Paton Electric Welding Institute (EWI) in Kiev has developed such methods as preliminary elastic deforming (PED) [4-5] or

higher frequency peening mechanical treatment (HFPMPT) [6] successfully used in structures made aluminium alloys or steels.

Typically, in thin-walled structures the sheet is joined with the reinforcing using welding from the rib side. In most cases two-sided fillet welds are made using automated TIG, EBW (electron beam welding) or LBW (laser beam welding) technologies. A more advantageous, yet more complicated solution is using (in such structure) welds with full penetration, made in one run from the sheet side, which melts the sheet fully and the rib partially.

The objective of the tests described was to develop a technology for welding stringer panels made of high strength VT-20 titanium alloy using slot welds and ensuring the obtainment of minimum internal stresses and strains and high service life indicators of such panels at cyclic loads.

The development of the technology for the strain-free welding of VT-20 alloy stringer panels was conducted at two stages. The first phase, involving the use of T-shaped specimens, was focused on investigating possible methods for welding the reinforcing rib to the sheet by means of the slot weld in combination with various technological procedures aimed at the improvement of manufacture accuracy and fatigue life of welded T-joints.

At the second stage, on the basis of technological variants developed at the first stage, a lot of ribbed panels were made. Afterwards, the panels were subjected to cyclic tension in order to confirm the possibility of manufacturing large-sized airplane panels meeting performance requirements without the use of heat treatment. The test T-joints and ribbed panels had geometrical dimensions corresponding to the structural parameters used in the manufacture of airplanes.

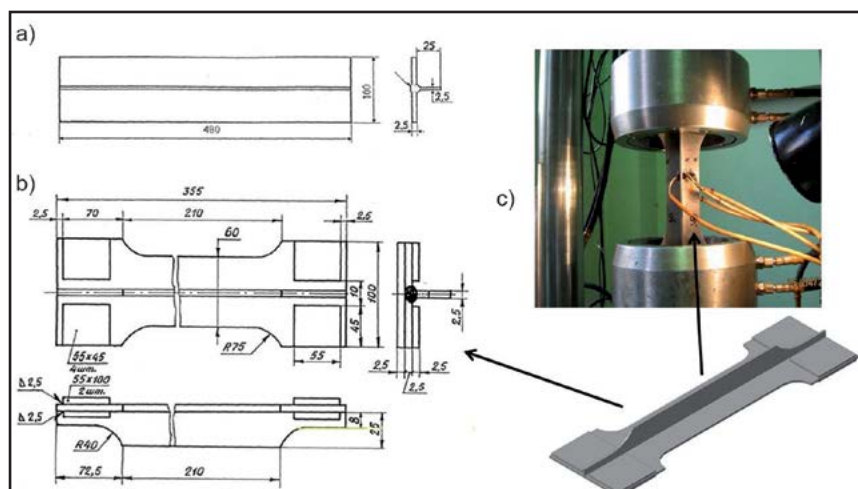


Fig. 1. Welded T-shaped specimen of the VT-20 alloy used at the first stage of tests: a – drawing of the welded specimen; b – drawing of the spade-shaped specimen for fatigue tests; c – specimen in the clamps of the fatigue testing machine

Within the first stage, tests experimentation-related T-joints were welded with one reinforcing rib (Fig. 1a) and next sampled for spade-like specimens (Fig. 1b) for fatigue tests. Figure 2 presents the structure of the ribbed panel with four welded stringers used at the second test stage along with the specimen cut out of it. Figure 3 presents a test rig for TIG welding of experimental ribbed T-joints and panels with slot welds in the condition of preliminary elastic deformation. The loading and fixing device enabled performing the preliminary tensile elastic deformation of the welded

sheets and ribs with the simultaneous bending of the sheet in the transverse direction. The test rig was equipped with a Fronius Magic Wave 3300 power source and a welding head with improved (additional) gas shielding of the arc and cooling weld. The welding head was moved using a triaxial manipulator and controlled by means of a programmable controller. The rig was also provided with a water cooling system and gas tooling.

At the first stage the following three welding methods were tested: automatic non-consumable electrode argon arc welding along the layer of activating flux (TIG-F), automatic non-consumable electrode argon arc welding with immersed arc (TIG-P) and electron beam welding in the vacuum chamber (EBW). The selection of these welding methods resulted from experience which the E.O. Paton Electric Welding Institute gained during welding titanium alloys but also was dictated by the necessity for the full melting of the sheet, failure-free melting of the sheet with the rib, the uniform weld root reinforcement from the rib side and the obtainment of weld face reinforcement without undercuts.

The TIG-P method is used for increasing the penetration depth and differs from the “classical” TIG method in the fact that the arc and the electrode tip are immersed in the weld pool under the sheet surface. The conditions of arc burning and those of metal motion in the weld pool differ significantly from those present during conventional TIG welding. The whole arc burns in a conical pit, the walls of which are washed with molten metal streams. This immersion maximises the efficiency of welding arc heat utilisation as well as intensifies hydrodynamic processes and heat exchange in the weld pool. However, the aforesaid phenomena are accompanied by a considerable increase in the thermal and electric load of the tungsten electrode tip.

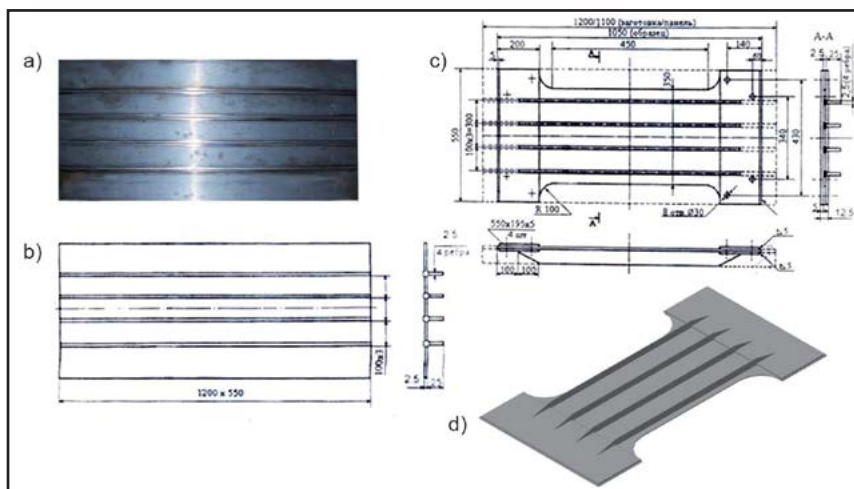


Fig. 2. Welded ribbed panel of the VT-20 alloy used at the second stage of tests: a) – main view of the welded panel; b) drawing of the welded panel; c) drawing of the spade-shaped specimen for tests; d) main view of specimen for fatigue tests



Fig. 3. Laboratory stand for TIG welding of ribbed panels in preliminary deforming conditions:  
 1 – gantry with the welding head travel car; 2 – control system; 3 – welding head; 4 – power source; 5 – loading system for preliminary elastic deforming of elements welded; 6 – welded panel

The EBW method is characterised by relatively high energy concentration and is usually used for welding thick elements. While making T-joints with full penetration, as opposed to the arc, the electron beam melts the sheet relatively easily thus ensuring the melting of the rib located under the sheet. At the same time the need for shaping the weld root reinforcement (up to 2 mm) from beneath the sheet from both sides of the rib is responsible for relatively restrictive limitations as regards the selection of welding parameters as it necessitates the weld pool extension from the face side.

The TIG-F method is intended for making welds 0.8÷6 mm thick titanium alloy sheets/plates [7]. Before welding, a flux layer is applied on the surface of the workpieces. Welding is performed in one run without scarfing. Supplying halide-based fluxes to the welding zone is responsible for blocking the arc in the peripheral zone caused by physical processes taking place in the arc. In such a situation the conditions for shaping the welded joint change significantly. Similarly, the technological possibilities of TIG-F welding extend considerably if compared with the conventional TIG welding method. The basic advantages of TIG-F welding include a greater penetration depth with significant decrease in the welding linear energy as well as the decrease in the weld width and that of HAZ.

The first stage of tests involved the determination of welding parameters using the T-joints with slot welds. Table 1 presents the parameters for all three methods used for welding VT-20 alloy.

The microstructures of the joints welded with the welding methods mentioned above are relatively similar. Figure 4

presents the macrostructure of the 2.5 mm thick T-joint TIG-F welded along the layer of the ANT-25A flux. The weld and HAZ are free from microcracks and gas pores. The HAZ was between 2.5 and 3 mm, whereas the weld width amounts to 6÷7 mm. In the weld, in the direction from the fusion zone to the welded joint centre it is possible to observe non-equiaxed grains, usually having the shape of columnar crystals packed with the heat off-take direction. In the central area of the weld it is possible to observe crystals of shapes close to equiaxed grains. The crystals merge in the weld centre, in the weld axis at angles of approximately 60÷90°. The grains in the weld are uniform in terms of size.

In order to obtain the weld excess metal it was necessary to use the VT1-00 filler metal wire having a diameter of 1.0 mm. The first stage of experiments involved determining the effect of the insertion of the wire into the weld pool on the reduction of alloying element contents

Table 1. Parameters for the three methods used in welding the VT-20 alloy

Welding method	EBW	TIG-F	TIG-P
Welding rate,m/h	14	18	17
Filler metal diameter, mm	1.0	1.0	1.0
Shield	vacuum 10-5	argon	argon
Electron beam current, mA	70		
Accelerating voltage, kV	28		
Focusing current, mA	80		
Oscillation amplitude, mm	8		
Oscillation frequency, Hz	380		
Current, A		195	250
Arc voltage, V		14.0-14.5	11.2-11.5

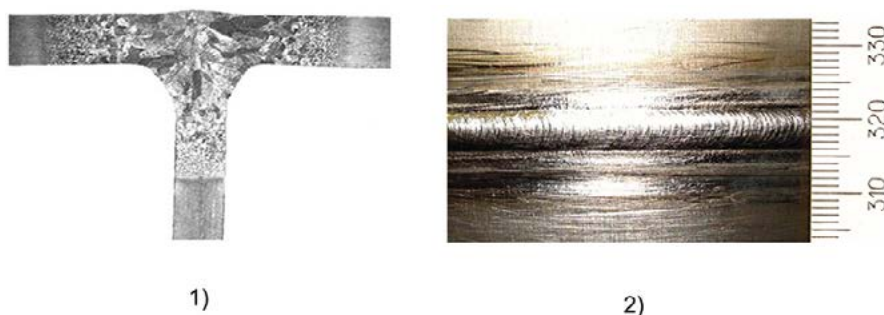


Fig. 4. Welded T-joint of the VT-20 alloy 2.5 mm thick: 1 – macrostructure; 2 – surface view from the face side

in the weld. The quantitative assessment of the weld metal alloying level was conducted using the X-ray spectral analysis. The contents of alloying elements, determined at selected points, varied within the following ranges 5.91÷6.33% Al; 1.65÷1.84% Zr; 0.77÷1.24% Mo; 1.06÷1.17% V, which corresponds to the contents of alloying elements in the VT-20 alloy.

In order to reduce welding residual stresses and strains it was necessary to use the plastic preliminary deformation of the elements welded. The sheet and the rib were subjected to longitudinal tension of a specific stress level. In addition, the sheet was subjected to bending in the direction opposite to the angular welding strains in the transverse direction.

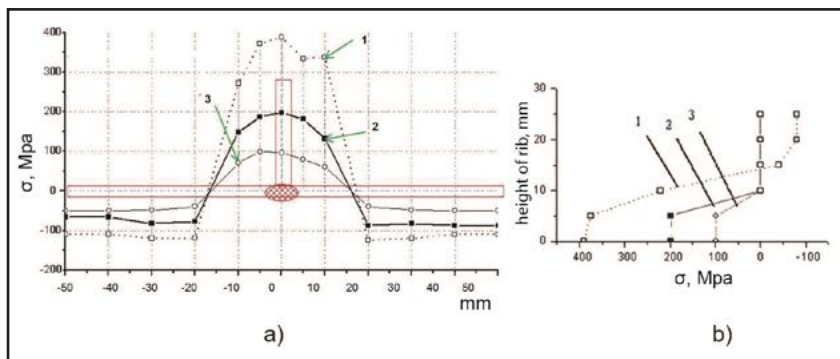


Fig. 5. Internal stresses in the T-shaped specimens of the VT-20 alloy with the EBW slot weld: 1 – welding of the specimen in the tooling without tension; 2 – welding of the specimen in longitudinal elastic tension conditions  $\sigma_{h,l} = 220$  MPa,  $\sigma_{h,p} = 250$  MPa; 3 – welding of the specimen in longitudinal elastic tension conditions  $\sigma_{h,l} = \sigma_{h,p} = 450$  MPa; a – in the sheet; b – in the rib.

In order to determine the optimum parameters of the longitudinal tension of the sheet and the rib, it was necessary to perform experiments aimed to determine the correlation between the internal stresses and plastic strains of the specimen and the preliminary tensile stresses. Figure 5 presents diagrams of the distribution of longitudinal internal stresses in the cross-section of the electron beam welded T-joint made at various initial stresses. It can be seen that the internal welding stresses decrease significantly along with increasing preliminary tensile stresses up to  $0.5\sigma_{0.2}$ . The internal stresses of the T-joint shape transformation (undulation)

also decrease along with increasing preliminary tensile stresses. After reaching the level of initial stresses amounting to  $0.3\div 0.35\sigma_{0.2}$ , the internal welding stresses of shape transformation practically do not exist.

The transverse bending of sheets in the opposite direction is used in order to fully remove the angular plastic strains. The size of the counter-bend was determined experimentally and amounted up to 0.75 of the angular plastic strains obtained while welding the test joint without fixing elements.

Five test joints out of each lot of the joints made using the three welding technologies mentioned above were subjected to heat treatment. Following the recommendations referring to

the manufacture of titanium alloy airplane structural components, the heat treatment was performed in the electric furnace in vacuum conditions with automatic temperature control. In order to prevent changes of the welded joint shapes during the heat treatment, a stainless steel stiffening device was used. The heat treatment parameters were the following: heating up to  $650^{\circ}\text{C}$  at a vacuum of  $1.33\cdot 10^{-1}$  MPa, a holding time of 2 hours and cooling with the furnace in vacuum.



Fig. 6. Treatment with the manual impact testing machine using HFPMT of the T-joint made of the VT-20 alloy; 1- specimen subjected to treatment; 2- impact testing machine head; 3-plate.

Five test joints out of each lot of the joints made using the three welding technologies mentioned above were subjected to higher frequency peening mechanical treatment (HFPMT) in order to increase the fatigue strength of the joints (Fig. 6). The peening mechanical treatment of the test joints consisted in peening the welded joint fusion zones both from the sheet and the rib side using an ultrasonic impact testing machine provided with high-melting beaters with rounded tips.

A present challenge related to making thin-walled light alloy structures is the development of repair welding technologies and the assessment of their effect on the strength usability of welded joints. Making T-joints using slot welds is connected with two characteristic types of imperfections. The first of them is the lack of smooth transition (rounding) from the sheet to the ring. The second is the presence of internal imperfections (gas pores, inclusions, microcracks). For this reason it was necessary to perform the assessment of efficiency of two repair

technologies. The removal of the first type of imperfections required smoothing of the transitions by means of TIG welding. The removal of the second type of imperfections required spot drilling from the face side followed sealing the opening using TIG welding with a filler metal. The repair welding was performed in a device fixing the specimen and providing the gas shielding for the sheet surface and rib. Following the repair the welded joints were subjected to HFPMT.

Before the tensile tests the specimens were fixed in the clamps of a URS-20 testing machine in the area of flat sections near the fronts (without the ribs, Fig. 1a) and subjected to longitudinal cyclic tensile load with the cycle asymmetry  $R_\sigma = 0.1$  at a frequency of 7 Hz. The tensile loads were selected so that the computational level of maximum cycle stresses in the sheet area (without the rib) amounted to  $0.5\sigma_{0.2}$  for the VT-20 alloy. However, in the load system presented above, the welded rib took over some part of the load imposed. As a result, the maximum

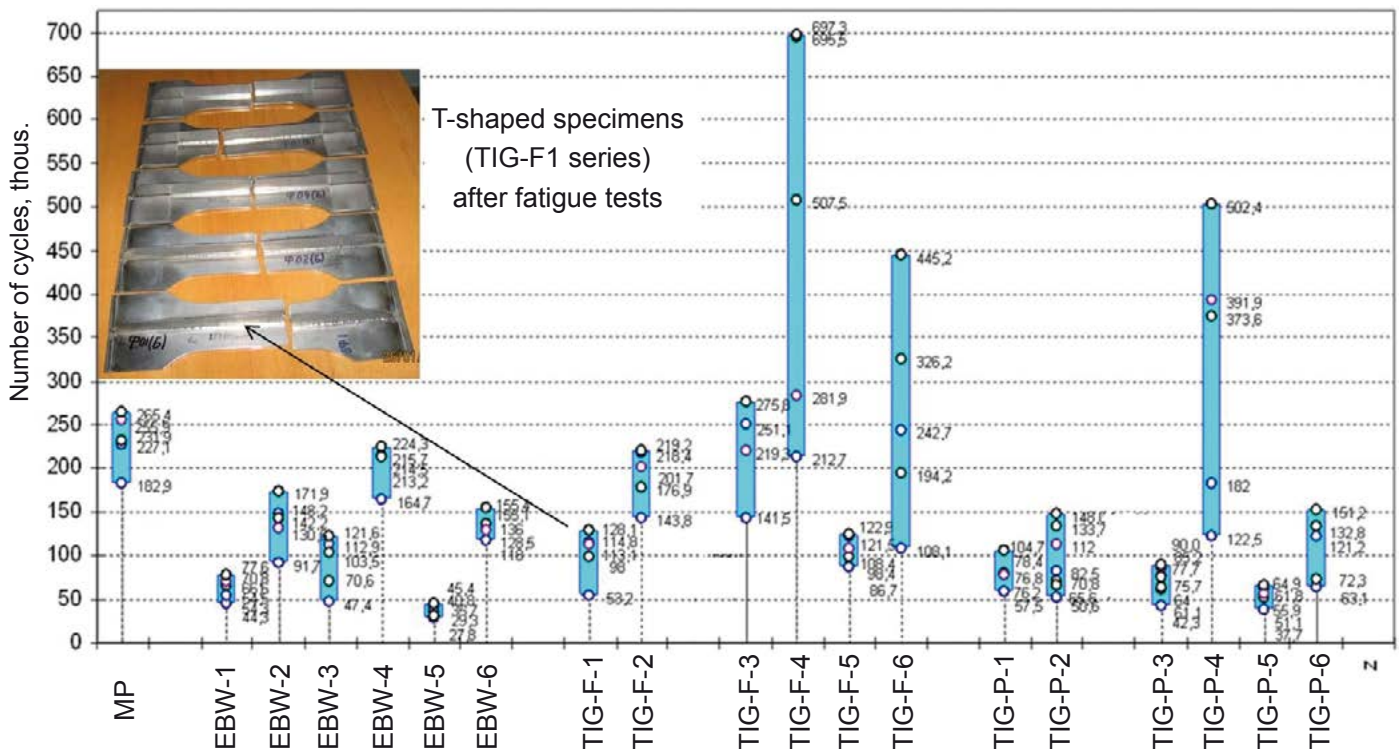


Fig. 7. Results of the fatigue tests at cyclic longitudinal tension of the T-shaped specimens made of the VT-20 alloy, with the specimens designated according to the welding method (EBW, TIG-F, TIG-P) and experimental conditions (PM – parent metal, 1 – during welding the specimens were stiffened in the tooling without tension, 2 – specimen subjected to longitudinal elastic tension, 3 – specimens with a smoothed weld leg, 4 – specimens subjected to treatment with the ultrasonic impact testing machine, 5 – specimens after the removal of imperfections, 6 – specimens after heat treatment)

cycle stresses in the net cross-section of the T-joint specimen were lower than those obtained in calculations. The determination of real stresses required the use of strain gauges. The measurements made using the strain gauges revealed the maximum strains in the central cross-section of the sheet to amount to 350 MPa.

The fatigue tests of the specimen were continued until a complete failure. The number of load cycles obtained was adopted as the assessment criterion concerning the variants of technologies and treatments applied.

Figure 7 presents the test results concerned with the T-shaped specimens used in the experiments of the first type. During the tests the specimens tended to fail in the 60 mm wide working cross-sections. The fatigue crack was formed in the area of transition from the weld to the parent metal and next propagated in both directions until the entire failure. The microfractographic examination of the fatigue fracture surface revealed that the failure in the slot weld zone tended to be ductile-brittle and ductile-quasi-brittle.

The joints subjected to the fatigue tests as the basic variants were the test T-joints made using each of the three welding methods without using the preliminary stretching (TIG-P-1, TIG-F-1, EBW-1 in Figure 7). As can be seen, the welding method affects the fatigue strength of the specimens tested. The lowest fatigue strength can be observed for EBW, whereas higher results can be seen using the TIG-P and TIG-F methods.

The preliminary elastic deforming doubles the cyclic fatigue strength of the welded joints (TIG-P-2, TIG-F-2, EBW-2) in comparison with the basic variants. Smoothing the weld legs decreases the cyclic fatigue strength of the welded joints obtained under conditions of the preliminary elastic tension for all the welding methods (TIG-P-3, TIG-F-3, EBW-3).

The higher frequency peening mechanical treatment of the welds made using the preliminary elastic tension significantly increases their load capacity, particularly while welding along

the layer of activating flux (specimens TIG-P-4, TIG-F-4, EBW-4).

The fatigue properties of the specimens decrease rapidly due to the repair of imperfections using the traditional TIG method from the sheet side (TIG-P-5, TIG-F-5, EBW-5). The specimens subjected to heat treatment (TIG-P-6, TIG-F-6, EBW-6) revealed significantly higher fatigue strength if welded along the layer of activating flux. However, it should be mentioned that the heat treatment is less effective if compared with the peening mechanical treatment of the welds by means of an ultrasonic impact testing machine.

The fatigue tests revealed that the greatest load capacity of the T-joints with the slot weld can be obtained using TIG-F and TIG-P welding with preliminary elastic tension and higher frequency peening mechanical treatment. For this reason the two technologies were used for welding tests at the second stage of the tests.

The second stage involved welding panels using the two selected methods, i.e. TIG-P and TIG-F. The technological parameters for welding the panels corresponded to the parameters of welding the test T-joints. The welding of the panels was performed using the preliminary elastic tension of the sheet and ribs amounting to  $\sigma_p = 220$  MPa and the counter-bend with a deflection of 14 mm. The welded joints of all the panels were subjected to higher frequency peening mechanical treatment using the tool and technology developed at the first test stage. It should be mentioned that due to the preliminary elastic deformation of the sheet and ribs the permanent panel shape changes were smaller than the initial bends of the sheets.

The quality control related to the welded joints involved the method of electron shearography [8] developed at the E.O. Paton Electric Welding Institute. This method enables the quick determination of unacceptable areas of the welded joints without the necessity of dismantling the loading tooling.

The fatigue tests of the welded panels required the preparation of large-sized spade-shaped specimens with the working part having the dimensions of 500×350×2.5 mm and edges subjected to grinding (Fig. 2d). The tests were performed using a Hydro-Puls-Schenk modernised versatile servo-hydraulic testing stand with the maximum tensile load of 100 tons and a 4-channel MTC Flex Test GT digital controller.

In order to reliably assess the actual level of stresses in the specimen working cross-section and to verify the correctness of specimen fixing in the testing machine clamps, the location of each specimen was calibrated using resistance strain gauges. To this end, on the surface of the specimen sheet and rib KF 5 P1-200 strain gauges were fixed and next connected to a SIIT-2 measurement system. The strain gauges were fixed in 3 cross-sections along the length of the working part (Fig. 8).

During the calibration, the panel specimen was subjected to the stepped tensile load with a step amounting to 5000 kgf/cm<sup>2</sup> until reaching the maximum value of the tensile load. For each step, the level of stresses was measured

using the strain gauges. The assessment was focused on the uniformity and the level of the maximum stresses on the strain gauges. In necessary cases the value of the maximum test load was corrected in order to create similar testing conditions for each panel. As a result, the maximum testing load was adjusted individually for each panel and restricted within the 30000 kgf/cm<sup>2</sup>÷32000 kgf/cm<sup>2</sup> range.

During the fatigue tests of the specimens, the frequency of the cyclic load amounted to  $f = 0.5$  Hz for the cycle asymmetry factor  $R = 0.1$ .

The diagram (Fig. 9) presents the test results related to the panels made using the TIG-P and TIG-F methods indicating the number of cycles preceding the failure. Panels made using the TIG method along the layer of activating flux are characterised by the highest fatigue strength.

The results obtained at the second stage of the tests revealed that the TIG welding with slot welds along the layer of activating flux with preliminary elastic deformation followed by higher frequency peening mechanical treatment can be used in the high-volume production of stringer panels made of the VT-20 grade titanium alloy.



Fig. 8. Panel with strain gauges fixed in the clamps of the fatigue testing machine

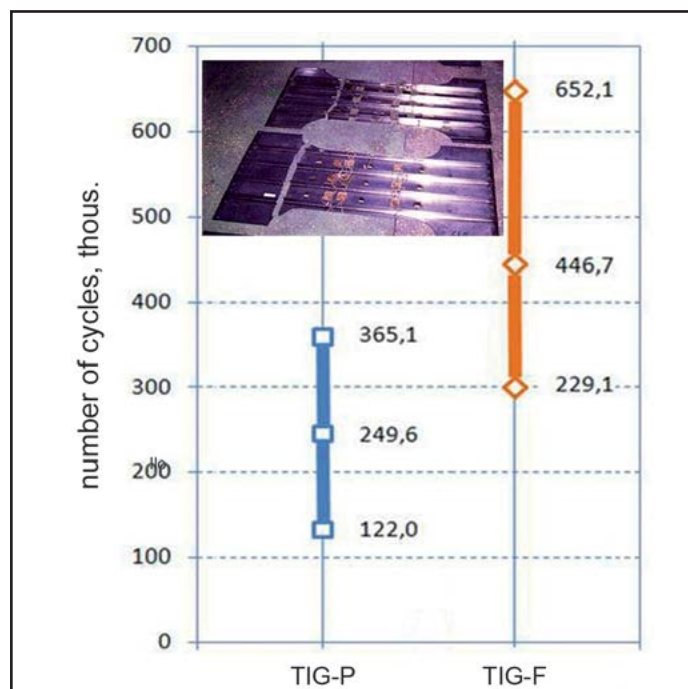


Fig. 9. Results of fatigue tests at cyclic longitudinal tension of the welded panels made of the VT-20 alloy, with the specimens designated according to the welding method (TIG-P and TIG-F)



## Conclusions

1. As a result of the complex tests conducted it was possible to state that making slot welds using the TIG-F welding along the layer of activating flux and applying the preliminary elastic deformation and high frequency peening mechanical treatment enables the obtainment of higher fatigue strength indicators for stringer panels made of the VT-20 high-strength titanium alloy if compared with those obtained while using electron beam welding or TIG-P welding with immersed arc.

2. The use of preliminary elastic deformation at the level not lower than  $0.25\sigma_{0.2}$  while welding large-sized VT-20 alloy stringer panels enables the elimination of welding residual strains in the form of undulation and improves automatic welding process conditions.

3. The use of high frequency peening mechanical treatment of welds is an effective manner of improving the fatigue strength of titanium alloy structures.

4. The technology developed enables making VT-20 alloy welded stringer panels without post weld heat treatment.

## References

1. Матвиенко С.В., Астафьев А.Р., Капасев И.Г. Сварка и родственные технологии в самолетостроении. Тенденции развития. Сварка в Сибири. 2003, № 2 (10), С.36-40.
2. Robert W. Messler JR. The Greatest Story Never Told: EB Welding on the F-14. Welding Journal, May 2007, pp.41-47.
3. Братухин А.Г. и др. Штамповка, сварка, пайка и термообработка титана и его сплавов в авиастроении. М.: Машиностроение, 1997. – 607с.
4. В. Е. Paton. Advanced trends in improvement of welded structures. Proceedings of international conference “Welding structures”, Kiev, Ukraine, 18-22 September, 1992, Welding and Surfacing Review, Harward Academic Publishers, 1992, Vol. 2, pp.1-18.
5. Lobanov L., Pavlovsky V. and Pivtorak V.A. Optical methods of studying and means of controlling welding strains and stresses. Soviet Technology Review. Section C. Welding and Surfacing Review, Harward Academic Publishers, 1992, p. 96.
6. Лобанов Л.М., Кирьян В.И., Кныш В.В., Прокопенко Р.И. Повышение сопротивления усталости сварных соединений металлоконструкций высокочастотной механической проковкой. (Обзор). Автоматическая сварка, 2006, С. 3-11.
7. Патон Б.Е., Замков В.Н., Прилуцкий В.П., Порицкий П.В. Контракция дуги флюсом при сварке вольфрамовым электродом в аргоне. Автоматическая сварка, 2000, № 1, С.2-9.
8. Лобанов Л.М., Пивторак В.А., Савицкая Е.М., Киянец И.В., Лысак В.В. Оперативный контроль качества сварных панелей из сплава VT-20 с использованием метода электронной широгрaфии. Автоматическая сварка, 2011, № 11, С. 28-33.